Electronic transport in carbon nanotube–graphene contact

Wuzhu Deng, Yang Li, Yangyang Chen, Wenli Zhou

School of Optical and Electronic Information, Huazhong University of Science and Technology, Wuhan 430074, People's Republic of China
E-mail: wlzhou@hust.edu.cn

Published in Micro & Nano Letters; Received on 13th May 2014; Revised on 8th July 2014; Accepted on 16th July 2014

An investigation has been conducted into the electron transport properties in carbon nanotube (CNT)–graphene contacts with a fully non-equilibrium Green's functions method combined with the density functional theory. Four different models are considered, where the contact geometries are varied. Their similar electron transmission characteristics are demonstrated with little dependence on the contact conditions at high energy and considerable dependence at low energy. The vacuum gap hinders the electron transport, resulting in an additional contact barrier. The electron transmission is mainly performed between the boundary carbon atoms of the CNT and the nearest graphene atoms, and the imperfection of the edge carbon atoms in a hexagonal lattice destroys the ballistic transport in graphene and the CNT at the contact. The current–voltage characteristics are presented as well. This reported work gives an insight into the electronic transport properties of the contacts and suggests that graphene is a suitable electrode material for applications in full-CNT devices.

1. Introduction: Carbon nanotubes (CNTs) and graphene have attracted great interest because of their unique electrical, optical, thermal and mechanical properties [1–5]. CNTs are promising candidates for nanoscale electronics, and some nanoelectronic devices based on individual CNTs have been studied, such as quantum wires, field-effect transistors, logic gates, field emitters, diodes, inverters and so on [6]. The performance of CNT devices crucially depends on the contacts between the CNT and the electrode [7, 8]. However, large electrical contact resistance between CNTs and a metal electrode hinders their practical electronics applications [7–9]. Graphene does not possess a bandgap [3], which makes it difficult to create graphene-based transistors with large on/off ratios, but its large electron mobility at room temperature and high mechanical strength makes it an ideal electrode material [3, 10]; for example, graphene is used to replace the expensive ITO electrode material in the solar cell [11, 12]. On the other hand, high-quality graphene can be fabricated with chemical vapour deposition on a wafer scale [13, 14].

Previous studies of CNT–metal contacts with first-principles calculation presented a Schottky barrier at the nanotube–metal interface [15, 16], which limits the electronic transport capability severely. High work-function metal contacts can reduce the Schottky barrier, but the height is still big (e.g. the reported lowest is ~0.4 eV for Pd) [17–19]. What is more, the metal wetting to the CNT is not perfect because the metal surface is not atom flat. An atomic-level physical gap exists between the CNT and the metal, inducing additional contact resistance [20, 21]. Graphene has similar chemical bonding to CNT, which makes it possible to be used as electrode material in CNT devices to minimise the contact resistance. Therefore the full advantageous transport properties of both graphene and nanotubes may be achieved. So far, only a few investigations on the properties of CNT–graphene contacts have been conducted [22–25]. The calculated Schottky barrier height of the contact is significantly lower than the reported metal electrodes, for example, it is 0.09 eV for (8, 0) nanotube–graphene contact [22], indicating that graphene is an excellent electrode material for semiconducting CNTs. Measurements with a graphitic interfacial layer inserted between the single-wall CNT and the metal electrode showed that the graphitic layer reduced the contact resistance as the wettability to the CNT was improved because of the formation of chemical bonding to the CNT [23]. However, another group claimed that graphene is not a suitable electrode candidate for transistor devices when studying few-layer graphene and larger nanotubes [24]. Nevertheless, the lack of detailed analysis on the contact geometry still makes it difficult to understand the electronic transport properties at the CNT–graphene contact.

In this Letter, self-consistent simulations are performed by non-equilibrium Green's functions (NEGFs) with a combination of density functional theory (DFT) [26, 27]. Calculations of electron transport from a CNT (8, 0) to a graphene sheet at their contact with different geometries are conducted, where the overlap length of the contact as well as the edge condition of the graphene and CNT (8, 0) are varied. On the basis of these models, we study the electronic transmission coefficients affected by the contact region length, the edge profile of the graphene sheet and the vacuum gap between the CNT and the graphene. Transmission spectrums and pathways are calculated to give another insight into the electronic transport properties. Current–voltage curves for the CNT (8, 0) in contact with graphene are discussed at the end of this Letter.

2. Calculation models: Four different CNT (8, 0)–graphene contact models are considered (see Fig. 1), consisting of three regions, that is, a graphene electrode, a CNT electrode and the central contact region linking them. In models (a), (b) and (c), the zigzag-edged graphene contact with the CNT is in the transverse transport direction and the graphene in model (d) is armchair-edged. The overlap length between the CNT and the graphene is 5 Å in (a), (b), (d) and 10 Å in (c). For comparison, the contact edge in (a), (d) is passivated by hydrogen. The vacuum gap of the graphene and CNT (8, 0) is set to 2.0 Å at first. All the models are optimised until the force on each atom in the contact region is less than 0.005 eV/Å. It appears that there is no covalent chemical bond formation between graphene and CNT atoms, suggesting that the π-conjugation of the graphene and the CNT in the contact models is not destroyed.

Their electronic transport properties are then calculated with fully self-consistent NEGF combined with DFT. The Perdew Burke Ernzerhof version of the generalised gradient approximation is adopted for the electronic exchange and correlation functional, and the valence electrons are expended in a numerical atom-orbital basic set of double zeta plus polarisation. Other technical parameters include a density mesh cutoff of 50 Hartree and the Brilloiun zones sampled with a $3 \times 3 \times 15$ grid of k points. A tolerance of 0.001 of the total energy is used as the convergence criterion.

doi: 10.1049/mnl.2014.0253

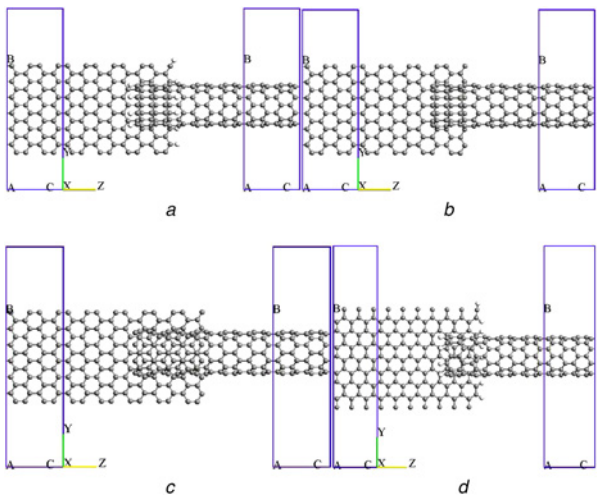

Figure 1 *Top view of four models investigated in this Letter*
Transport direction is along the *Z* direction and the vacuum gap between CNT (8, 0) and graphene is 2 Å
CNT (8, 0) is on the top of graphene
a, *b* Zigzag-edged graphene with 5 Å overlap; terminal edge of (a) is passivated by hydrogen atoms
c Zigzag-edged graphene with 10 Å overlap
d Armchair-edged graphene with 5 Å overlap and hydrogen-passivated terminal edge

3. Results and discussion: The calculated transmission coefficient without bias for the individual zigzag-edged graphene, the CNT (8, 0) and model (a) are shown in Fig. 2*a*. The transmission gap of the CNT (8, 0) is located between −0.28 and 0.27 eV, which agrees with its bandgap of 0.55 eV by experiment [28]. For model (a), the transmission gap of the CNT (8, 0) is retained, which indicates that the CNT (8, 0) retains its semiconducting nature and a very low barrier in the CNT (8, 0)–graphene contact. Another transmission valley presents at the energy range of [0.42–1.02] eV, where the electron transport is suppressed by scattering. The transmission coefficient is decreased compared with the individual CNT (8, 0) or graphene, this is because there is no chemical bond formation between graphene and CNT atoms, and this destroys the ballistic transport in the CNT and graphene.

The transmission coefficients at zero bias for the aforementioned four contact models are plotted in Fig. 2*b*. We can note that the transmission coefficients have the same transmission gap near the Femi level, and the energy range $E = [-0.28–0.27]$ eV agrees with the bandgap of the CNT (8, 0). Meanwhile, the amplitudes of the transmission spectrums and their peak positions are quite similar although the transmission coefficients of each model are not exactly the same. However, transmission coefficients of contacts without the hydrogen-passivated terminal edge in models (b) and (c) have more resonance peaks in the energy range [−1.10 to −0.48] eV, which means that the hydrogen-passivated terminal edge contact as models (a) and (d) are more at equilibrium. For contact with 10 Å overlap, the transmission coefficient is smaller in the energy range [0.27 to 1.02] eV, but changes little in other energy ranges. Their little dependence on the contact conditions at high energy and considerable dependence at low energy suggests that all-carbon CNT-based devices with the graphene electrode are feasible. It is obviously more practical for those CNT devices which usually work at high bias to adopt the graphene electrode without considering the edge geometry, for example, thermal-based sensors like flow sensors [29], actuators like microbubble generators [30] and so on.

Some experiments have disclosed that the contact resistance is large for the metallic CNT and metal contact [10], where the Schottky barrier should not exist. Besides, there is additional contact resistance for the atomic-level physical gap, which exists between the CNT and the metal, and the cohesion is inversely correlated with the metal–carbon vacuum gap [31]. To investigate the vacuum gap effects on the transmission property of the CNT–graphene contact, we shifted the vacuum gap from 2 to 3.35 Å. Subjected to the same preceding technical parameters, the resultant transmission spectrums are shown in Fig. 2*c*. The transmission spectrums are similar but model (c) obviously has peaks at −0.57 and 0.37 eV. By comparison with the vacuum gap 2 Å, a trend can be deduced, that is, the bigger the gap in the contact, the smaller the transmission coefficient.

To achieve further investigation, the electron transmission pathway and current density of contact model (a) at energy of 1.6 eV is calculated, where the potential is 0.8 V left and −0.8 V right. As shown in Fig. 3, the incident electrons transmit through the CNT along the device direction to the graphene at each bond and atom. Red arrows denote electron transfer pathways, showing that electron transmission from the CNT to the graphene is mainly performed between the nearest boundary carbon atoms. In addition, electrons transferring from hydrogen atoms to carbon atoms contribute little to the current flow, but keep the contact more at equilibrium. The current density in the CNT drops at the boundary contacting the graphene sheet, which is because the imperfection of the edge carbon atoms in a hexagonal lattice generates contact resistance, and destroys the ballistic transport in the graphene and the CNT when electrons transfer through the contact. The result is coincident with the transmission coefficient decreasing at the

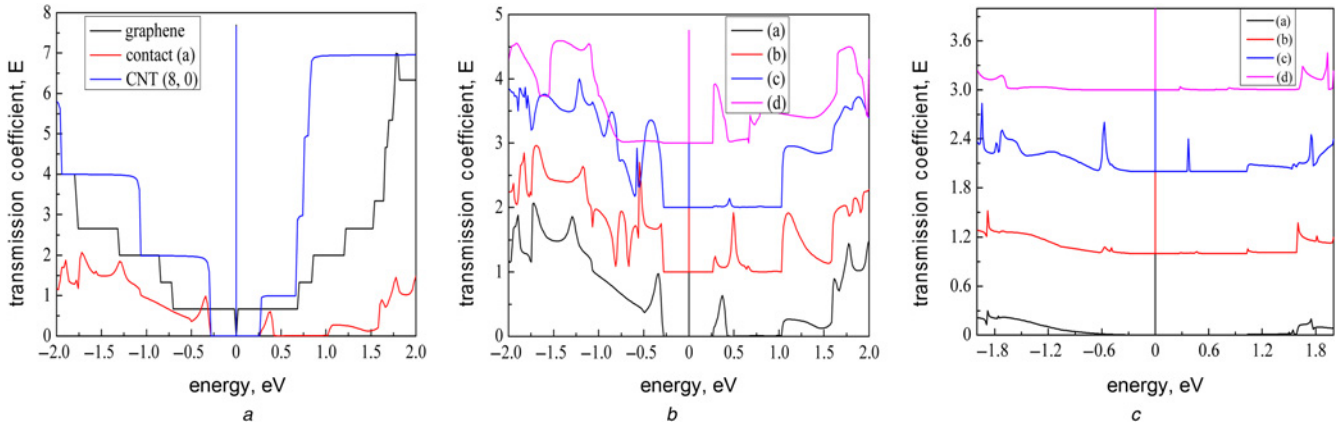

Figure 2 *Transmission coefficient at zero bias for individual zigzag-edged graphene, CNT (8, 0) and model (a) (Fig. 2a); for four different models with vacuum gap 2 Å (Fig. 2b); for four different models with vacuum gap 3.35 Å (Fig. 2c)*

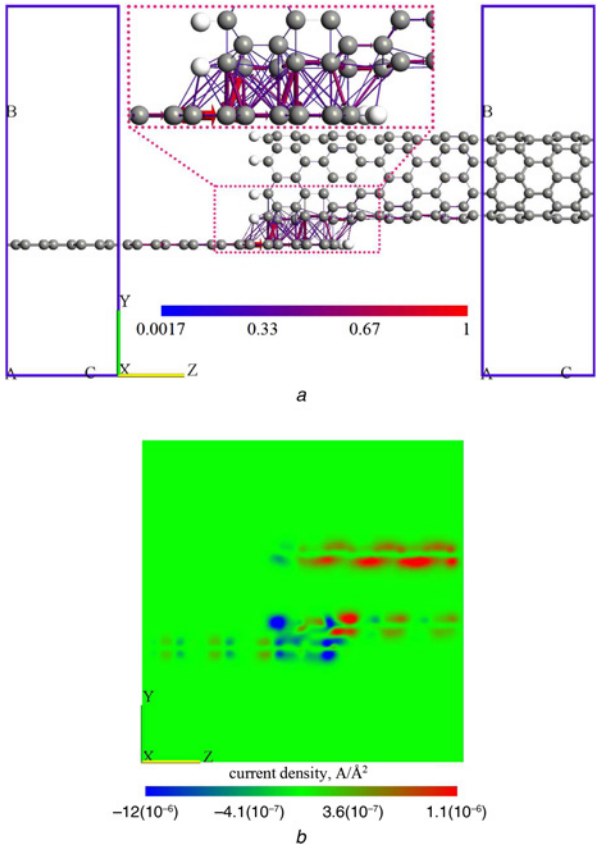

Figure 3 *Transmission pathway of model (a) in Fig. 1 at energy 1.6 eV (Fig. 3a) (arrows stand for main electron transfer pathways), inset shows magnified contact region; current density of model (a) at bias of 1.6 V along Z direction, averaged in X direction (Fig. 3b)*

contacts. On the basis of the above certain specifications, our current simulation results demonstrate that contact overlap has little effect on the electron transport and graphene is a promising excellent electrode to construct all-carbon CNT devices.

The above self-consistent calculations at different bias and the transmission spectrums indicate the probability that the electron with incident energy E is transferred from the left graphene electrode to the right nanotube electrode. The integration of the transmission spectrum yields the electric current [27], and the current–voltage (I–V) curve of model (a) as an example is shown in Fig. 4. There is barely current through the contact at low bias, but the current increases at high bias. This remains the transport nature of semiconducting CNTs. A curve 'step' appears at a bias of about 0.9–1.4 V. The current at higher bias is more than 20 μA, which is larger than that in the model with a bigger vacuum gap, for example, 3 Å, in accordance with the tendency in transmission coefficients.

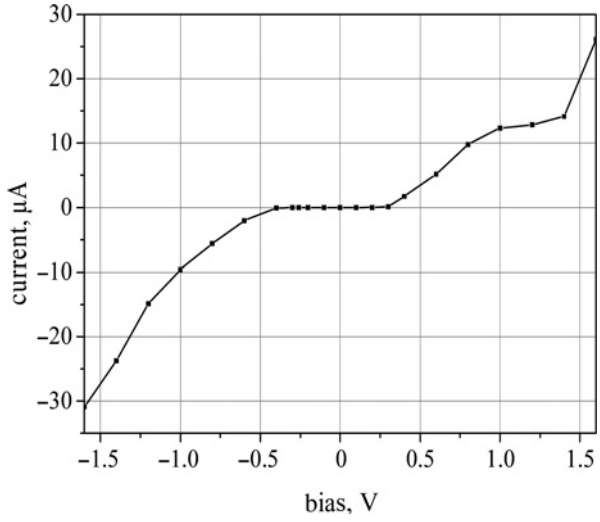

Figure 4 *Current–voltage curve of CNT–graphene contact model (a)*

4. Conclusion: In summary, we have employed NEGFs with a combination of DFT to investigate the electronic transport properties of the CNT–graphene contact with geometry effects. It is found that the covalent bond is difficult to form in the contact. Electron transmission coefficients are similar with little dependence on the contact conditions at high energy, but it is sensitive at low energy. On the other hand, the vacuum gap makes an additional contact barrier and hinders electron transport. Electron transmission mainly occurs between the boundary carbon atoms of the CNT and the nearest graphene atoms, but non-chemical bonding destroys their ballistic transporting. Our work gives a useful insight into the electron transport properties of the contact and suggests that the contact can be used at high bias without considering the edge geometry. Therefore graphene is a better electrode material than metal for CNT devices in the circumstances and corresponding full carbon devices can be expected.

5. Acknowledgments: This work was supported by the National Natural Science Foundation of China (no. 61274115), the Major National Scientific Instrument and Equipment Development Project (no. 2011YQ160002) and the China Scholarship Council.

6 References

[1] Castro Neto A.H., Guinea F., Peres N.M.R., Novoselov K.S., Geim A.K.: 'The electronic properties of graphene', *Rev. Modern Phys.*, 2009, **81**, pp. 109–162
[2] Novoselov K.S.: 'Nobel lecture: graphene: materials in the flatland', *Rev. Modern Phys.*, 2011, **83**, pp. 837–849
[3] Geim A.K., Novoselov K.S.: 'The rise of graphene', *Nat. Mater*, 2007, **6**, pp. 183–191
[4] Kong J., Yenilmez E., Tombler T.W., *ET AL.*: 'Quantum interference and ballistic transmission in nanotube electron waveguides', *Phys. Rev. Lett*, 2001, **87**, p. 106801
[5] Rosenblatt S., Yaish Y., Park J., Gore J., Sazonova V., McEuen P.L.: 'High performance electrolyte gated carbon nanotube transistors', *Nano Lett.*, 2002, **2**, (8), pp. 869–872
[6] Ajayan P.M., Zhou O.Z.: 'Applications of carbon nanotubes', *Carbon Nanotubes*, 2001, **80**, pp. 391–425
[7] Shan B., Cho K.: 'Ab initio study of Schottky barriers at metal-nanotube contacts', *Phys. Rev. B*, 2004, **70**, p. 233405
[8] Heinze S., Tersoff J., Martel R., Derycke V., Appenzeller J., Avouris P.: 'Carbon nanotubes as Schottky barrier transistors', *Phys. Rev. Lett.*, 2002, **89**, p. 106801
[9] Kim W., Javey A., Tu R., Cao J., Wang Q., Dai H.J.: 'Electrical contacts to carbon nanotubes down to 1 nm in diameter', *Appl. Phys. Lett.*, 2005, **87**, (17), pp. 173101–173103
[10] Morozov S.V., Novoselov K.S., Katsnelson M.I., *ET AL.*: 'Giant intrinsic carrier mobilities in graphene and its bilayer', *Phys. Rev. Lett.*, 2008, **100**, p. 016602
[11] Wang X., Zhi L., Mullen K.: 'Transparent, conductive graphene electrodes for dye-sensitized solar cells', *Nano Lett.*, 2007, **8**, (1), pp. 323–327
[12] Eda G., Fanchini G., Chahowalla M.: 'Large-area ultrathin films of reduced graphene oxide as a transparent and flexible electronic material', *Nat. Nano.*, 2008, **3**, (5), pp. 270–274
[13] Li X., Cai W., Colombo L., Ruoff R.S.: 'Evolution of graphene growth on Ni and Cu by carbon isotope labeling', *Nano Lett.*, 2009, **9**, (12), pp. 4268–4272
[14] Li X., Magnuson C.W., Venugopal A., *ET AL.*: 'Large-area graphene single crystals grown by low-pressure chemical vapor deposition of methane on copper', *J. Am. Chem. Soc.*, 2011, **133**, (9), pp. 2816–2819

doi: 10.1049/mnl.2014.0253

[15] Svensson J., Campbell E.E.B.: 'Schottky barriers in carbon nanotube-metal contacts', *J. Appl. Phys.*, 2011, **110**, p. 111101
[16] Zhu W., Kaxiras E.: 'Schottky barrier formation at a carbon nanotube–metal junction', *Appl. Phys. Lett.*, 2006, **89**, p. 243107
[17] Liang W., Bockrath M., Bozovic D., Hafner J.H., Tinkham M., Park H.: 'Fabry-Perot interference in a nanotube electron waveguide', *Nature*, 2001, **411**, pp. 665–669
[18] Javey A., Guo J., Wang Q., Lundstrom M., Dai H.: 'Ballistic carbon nanotube field-effect transistors', *Nature*, 2003, **424**, pp. 654–657
[19] Chen Z., Appenzeller J., Knoch J., Lin Y., Avoures P.: 'The role of metal–nanotube contact in the performance of carbon nanotube field-effect transistors', *Nano Lett.*, 2005, **5**, (7), pp. 1497–1502
[20] Lee S., Kahng S.J., Kuk Y.: 'Nano-level wettings of platinum and palladium on single-walled carbon nanotubes', *Chem. Phys. Lett.*, 2010, **500**, (1–3), pp. 82–85
[21] Zhang Y., Franklin N.M., Chen R.J., Dai H.J.: 'Metal coating on suspended carbon nanotubes and its implications to metal-tube interaction', *Chem. Phys. Lett.*, 2000, **331**, (1), pp. 35–41
[22] Cook B.G., French W.R., Varga K.: 'Electron transport properties of carbon nanotube–graphene contacts', *Appl. Phys. Lett.*, 2012, **101**, p. 153501
[23] Chai Y., Hazeghi A., Takei K., *ET AL.*: 'Low-resistance electrical contact to carbon nanotubes with graphitic interfacial layer', *IEEE Trans. Electron Devices*, 2012, **59**, pp. 12–19
[24] Pei T., Xu H., Zhang Z., *ET AL.*: 'Electronic transport in single-walled carbon nanotube/graphene junction', *Appl. Phys. Lett.*, 2011, **99**, p. 113102
[25] Paulson S., Helser A., Nardelli M.B., *ET AL.*: 'Tunable resistance of a carbon nanotube-graphite interface', *Science*, 2000, **290**, pp. 1742–1744
[26] Ouyang F., Hui X., Fan T.: 'All-carbon nanoswitch based on C 70 molecule: a first principles study', *J. Appl. Phys.*, 2007, **102**, p. 064501
[27] Li Z., Kosov D.S.: 'Dithiocarbamate anchoring in molecular wire junctions: a first principles study', *J. Phys. Chem. B*, 2006, **110**, (20), pp. 9893–9895
[28] Odom T., Zhang J., Kim P., Lieber C.: 'Atomic structure and electronic properties of single-walled carbon nanotubes', *Nature*, 1998, **391**, pp. 62–65
[29] Ouyang M., Li W.J., Leong P.H.W., Wong K.W.: 'Improving carbon nanotubes sensor time response and responsivity using constant-power activation', *IEEE Trans. Nanotechnol.*, 2012, **11**, (3), pp. 624–632
[30] Zhou W., Li Y., Sun W., Wang Y., Zhu C.: 'Characteristics of carbon nanotubes based micro-bubble generator for thermal jet printing', *J. Nanosci. Nanotechnol.*, 2011, **11**, pp. 10525–10529
[31] Matsuda Y., Deng W., Goddard W.A.: 'Contact resistance properties between nanotubes and various metals from quantum mechanics', *J. Phys. Chem. C*, 2007, **111**, (29), pp. 11113–11116